EFFECT OF SiO$_2$-CaO-Cr$_2$O$_3$ ON THE CREEP PROPERTY OF URANIUM DIOXIDE

YOUNG WOO RHEE*, KI WON KANG, KEON SIK KIM, JAE HO YANG, JONG HEON KIM and KUN WOO SONG
Korea Atomic Energy Research Institute
150 Deokjin-dong, Yuseong-gu, Daejeon, Korea, 305-354
*Corresponding author. E-mail : youngwoo@kaeri.re.kr

πThe effects of silica-based additives have been investigated to improve the creep property of a UO$_2$ pellet. The additive composition, 50wt%SiO$_2$-47wt%CaO-3wt%Cr$_2$O$_3$ (SCC), was selected according to the dihedral angle and the distribution of the second phase. It was observed that the creep rate of the 0.07 wt% SCC-added UO$_2$ was slower than that of the pure UO$_2$. However, the creep rate of the 0.22 wt% SCC-added UO$_2$ was about 3.48 times faster than that of the pure UO$_2$, depending on the applied stress in the lower stress range. In the case of the 0.35 wt% SCC-added UO$_2$, the creep rate decreased in comparison with that of the 0.22 wt% SCC-added UO$_2$. The observed enhancement in the creep rate might depend on a balance between the positive role of the viscous intergranular phase and the negative roles of the additives and the grain growth.

1. INTRODUCTION

Uranium dioxide, one of the most important nuclear fuel materials, is used in nearly all commercial nuclear power plants. The UO$_2$ fuel irradiated in a reactor suffers both volume shrinkage, due to in-reactor densification, and volume expansion, due to the accumulation of fission products. Volume shrinkage dominates in the range of lower burnups, for example, of less than 10000 MWD/MTU; however, volume expansion dominates in the range of higher burnups. The swelling occurs because of the accumulation of fission products, and thus the fuel volume increases with the burnup.When the UO$_2$ fuel contacts the cladding, the swelling of the fuel puts a mechanical load onto the cladding. An excessive load could lead to cladding failure, i.e., PCI (pellet-clad-interaction) failure. To reduce the likelihood of such a PCI failure, it has been recommended that the UO$_2$ fuel, rather than the cladding, be made to deform easily at the service temperature, because the UO$_2$ fuel is much harder than the metal cladding. Accordingly, UO$_2$ fuel with a high creep rate is required.

Over the last 30 years, many studies have reported on the creep property of uranium dioxide [1-4]. Most of these studies have shown that the creep rate of uranium dioxide follows the power laws characterized by two different stress exponents: an order of roughly 1 at low stresses and an order of 3 to 8 at high stresses [3]. At low

stresses, stress-directed diffusion is usually the dominant creep mechanism. The larger stress exponents at high stresses indicate that the UO$_2$ pellet deforms by dislocation creep. The transition stress between the two regions decreases with increasing grain size or O/U ratio [4].

For stoichiometric and hyperstoichiometric UO$_{2+x}$, the steady-state creep rates increase with an increasing nonstoichiometry [5,6] and a decreasing grain size [3,7-9]. Under low stresses, the steady-state creep rates for UO$_{2+x}$ increase linearly with nonstoichiometry, x. Creep rates for UO$_{2+x}$ at high stresses show an $x^{1.75}$ to x^2 dependence for polycrystals and an x^2 dependence for single crystals. Nearly all studies on the relationship between the creep rate and the grain size, d, show an $\dot{\varepsilon} \propto d^{-2}$ dependence, except for the study by Chung and Davies [9] who reported that the creep rate dependence varies from d^{-2} to d^{-3} with decreasing grain size.

However, these two material properties significantly affect other important fuel performances. For example, a small grain size leads to a large fission gas release, which is deleterious for fuel performance at a high burnup. The O/U ratio should be restricted to a specific range of 2.0 ± 0.01, because the thermal conductivity of the UO$_2$ pellet decreases with an increasing nonstoichiometry. Thus, the controls of grain size or nonstoichiometry are inappropriate ways to enhance the creep properties of UO$_2$ pellets.

UO$_2$ creep is very sensitive to the presence of impurities, because impurities can alter the effective

stoichiometries and the diffusivities of UO_2. Armstrong and Irvine [10] found that small additions (< 1%) of CaO, Y_2O_3, or ZrO_2 reduced the creep rate ten-fold by solid solution hardening and increased the apparent activation energy for creep. Recently, Delafoy et al. [11] reported that the addition of Cr_2O_3 significantly increases the rate of deformation of UO_2 in the high-stress range.

Second phase can be precipitated when a large amount of added impurities exceeds the solubility limit. The addition of SiO_2, caused an amorphous second phase at the grain boundaries and increased the creep rate of UO_2. [12] Lay et al. [13,14] reported that the glassy aluminosilicate or magnesium aluminosilicate phase increased both the grain size and the creep rate of the UO_2 pellet. Kang et al. [15] showed that a $NiO-SiO_2$ additive formed spherical precipitates in the grain boundaries and thereby increased the creep rate in the high stress region. Bibilashvili et al. [16] found that co-doping of aluminosilicate and Nb_{2O5} enhanced the creep rate of UO_2 and reduced the fuel-cladding mechanical interaction.

It is well known that creep of ceramic materials strongly depends on the properties of the grain boundary phase, such as distribution, wetting behavior, volume fraction, and crystallinity. [17] Generally, a wetted amorphous grain boundary phase enhances the creep rate of ceramic materials. The creep rate is known to increase in proportion to the cube of the nominal volume fraction of a glassy phase for a linear viscous glassy phase in a polycrystal containing an amorphous grain boundary phase. The crystallization of the amorphous grain boundary phase usually increases the creep resistance of ceramic materials. The composition of the second phase could affect considerably the properties of the grain boundary phase. However, only the effects of MgO, Al_2O_3 [13,14], and Nb_2O_5 [16] in the SiO_2-based second phase in UO_2 pellets have been studied.

The purposes of the present investigation are (1) to find a new intergranular phase that can enhance the UO_2 creep rate and (2) to evaluate the effects of this novel phase on both the microstructure and the creep rate. The SiO_2-CaO-Cr_2O_3 system was selected from among four candidate systems, SiO_2-ZnO, SiO_2-CaO-Cr_2O_3, SiO_2-MnO, and SiO_2-Y_2O_3-Cr_2O_3, by means of a screening test, which covered the distribution of the intergranular glassy phase and the wetting behavior. The creep properties of the SiO_2-CaO-Cr_2O_3-added UO_2 pellet were compared with those of pure UO_2.

2. EXPERIMENTAL PROCEDURE

The additives were determined using two criteria: a lower melting point than the sintering temperature and glass forming abilities. The compositions of the additives chosen were $51SiO_2$-49ZnO, $50SiO_2$-47CaO-3Cr₂O₃, $51SiO_2$-49MnO, and $42SiO_2$-53Y₂O3-5Cr₂O₃ in weight

percentages from the phase diagrams. Additive powders were ground in ethanol by ball-milling with zirconia balls for 12 h and then dried. As a screening test, ADU-UO_2 powder and 1 wt% of the dried additives were sieve-mixed three times and then compacted under 3 tons/cm². The powder compacts were calcined at 900°C for 1 h in H_2 and then sintered at 1700°C for 4 h in a gas mixture of H_2-5%CO_2. The sintered samples were ground and polished to a 1-μm finish. The microstructures of the sintered samples were observed along their polished sections using an optical microscope. The distribution and the wetting of the intergranular glass phase showed the best behavior with the additive of $50SiO_2$-47CaO-3Cr₂O₃. Therefore, this additive composition was ultimately selected. (see Fig. 1)

The samples for the compression creep test were prepared in the same way using 0.07, 0.22, and 0.35 wt% of the $50SiO_2$-47CaO-3Cr₂O₃ additive, respectively. The samples were of a cylindrical geometry, ~8 mm in height and ~8 mm in diameter. The sintered density was measured using the water immersion method. All the samples were limited to a density of 95.5±1 %TD using 0.3 wt% of the pore former azodicarbonamide. EDS (Energy dispersive spectroscopy) and XRD (X-ray diffraction) analysis were preformed on the polished surfaces of the sintered samples. The grain sizes of the polished samples were measured using the linear intercept method after being etched at 1300°C for 1 h in CO_2. The compression creep tests were conducted in a dead load system with a tungsten heating element furnace. The tests were carried out in an Ar-5% H_2 atmosphere under 20, 35, 50, and 65 MPa at 1500°C. The pure UO_2 samples, the reference samples, were also made and tested in the same way.
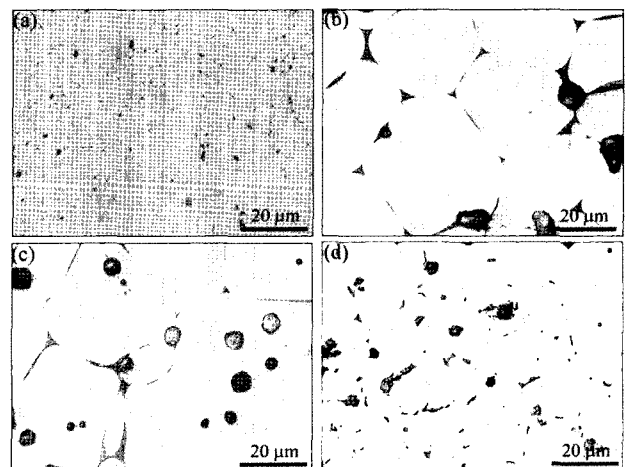

Fig. 1. Pore Structures of the UO_2 Pellets Added with 1 wt% of (a) $51SiO_2$-49ZnO, (b) $50SiO_2$-47CaO-3Cr₂O₃, (c) $51SiO_2$-49MnO and (d) $42SiO_2$-53Y₂O₃-5Cr₂O₃

3. RESULTS AND DISCUSSION

Figure 1 shows the pore structures of the sintered UO$_2$ pellets containing 1 wt% of four kinds of additives, 51SiO$_2$-49ZnO, 50SiO$_2$-47CaO-3Cr$_2$O$_3$, 51SiO$_2$-49MnO, and 42SiO$_2$-53Y$_2$O$_3$-5Cr$_2$O$_3$ as weight percentages.

Among the four candidate additive systems, the 50SiO$_2$-47CaO-3Cr$_2$O$_3$-added sample shows well-dispersed second phases and a small dihedral angle. In the case of the 51SiO$_2$-49ZnO-added sample, the second phase was not observed. This could be attributed to the high vapor pressure of ZnO, 1387 Pa at 1500°C. The 51SiO$_2$-49MnO-added sample also shows well-dispersed second phases and a small dihedral angle, but the density of the sintered pellet was

much lower than the required value, being around 95%TD. In the 42SiO$_2$-53Y$_2$O$_3$-5Cr$_2$O$_3$-added sample, the second phases were well-dispersed in the triple junctions. However, the dihedral angle of this sample is larger than that of the 50SiO$_2$-47CaO-3Cr$_2$O$_3$-added sample. Thus, the 50SiO$_2$-47CaO-3Cr$_2$O$_3$ system (hereafter called SCC) was selected as the new composition for the additive.

The phase diagram of the selected additive system is shown in Fig. 2. The melting point of the selected additive was estimated to be about 1540°C, as shown in Fig. 2. Therefore, the SiO$_2$-based additive formed a liquid phase at the sintering temperature and then the liquid phase vitrified to a glassy phase during the cooling step because of the large viscosity of the SiO$_2$-based liquid.

The sintered density and the grain size of the SCC-added samples are illustrated in Fig. 3. The sintered densities were 95.5 %TD, 95.4 %TD, and 94.6 %TD for 0.07 wt%, 0.22 wt%, and 0.35 wt% of the SCC additives, respectively. The grain size was around 8 μm in both the 0.07 and 0.22 wt% added samples but significantly increased to 24 mm in the 0.35 wt% added sample. A liquid phase can provide a rapid medium for material transport during sintering and can cause fast grain growth. The larger grain size of the 0.35 wt% added sample might be attributed to the much larger amount of liquid phase than those of the other two compositions (See Fig. 4).

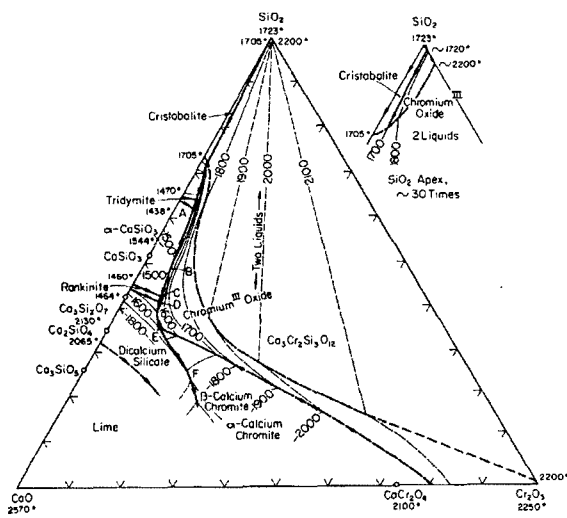Figures 4(a)-4(c) show the grain structures of the SCC-added samples for various additive contents. The

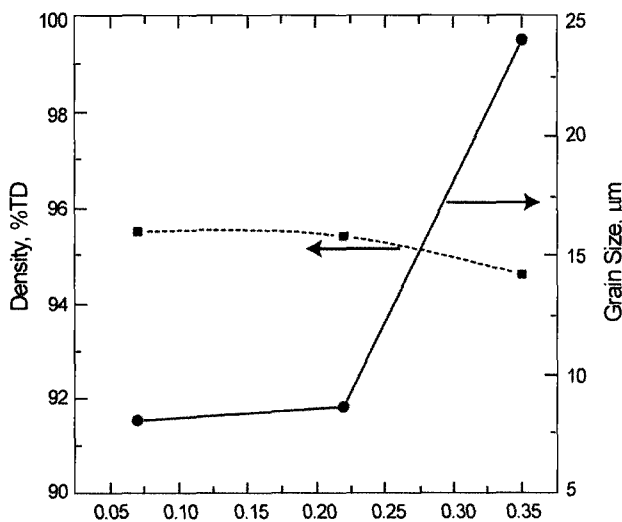Fig. 2. Phase Diagram of the SiO$_2$-CaO-Cr$_2$O$_3$ System [16]

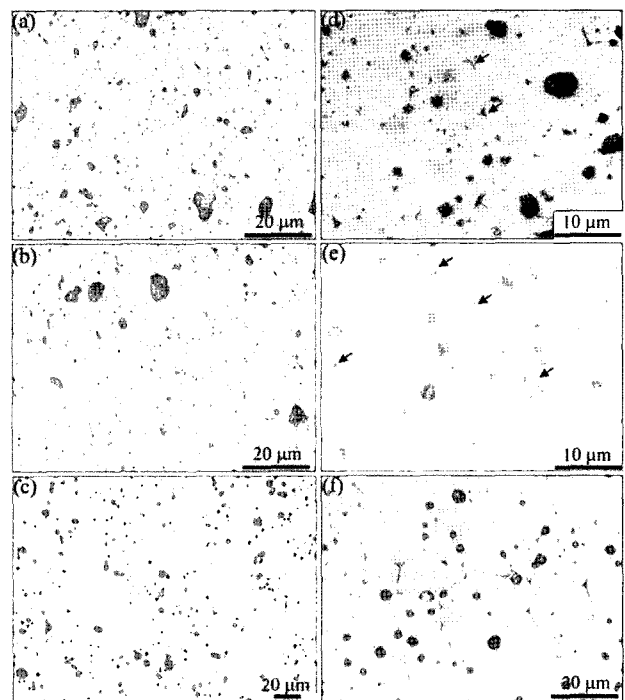Fig. 3. Relative Densities and Grain Sizes with the Various Contents of the SCC Additive

Fig. 4. Grain Structures and Pore Structures of the SCC-added Samples; 0.07wt% (a,d), 0.22wt% (b,e) and 0.35wt%(c,f). Arrows Indicate the Intergranular Phases

grain size of the 0.35 wt% added sample is much larger than those of the 0.07 and 0.22 wt% added samples. Figures 4(d) and 4(e) show that the second phase is mostly found at the triple junctions in the samples with a lower additive content. The pore structure of the 0.35 wt% added sample shows a well-dispersed second phase at the grain boundaries and the triple junctions (See Fig. 4(f)). The pore size of the 0.35 wt% added sample is larger than those of the 0.07 and 0.22 wt% added samples. Thus, the slightly lower density of the 0.35 wt% added sample could be attributed to the fast grain growth and the pore coalescence during sintering. Figure 5 shows the XRD patterns of the SCC-added samples for various additive contents. All the peaks in Fig. 5 are those of the UO_2 phase and no crystalline phase is found except for UO_2. It appears that the second phases shown in Fig. 4 are amorphous glassy phases.

The steady state creep rates for the SCC-added samples are shown as a function of the applied stress in Fig. 6 and are compared with the steady state creep rate of pure UO_2. In each deformation regime, the creep rate can be expressed using a power law:

$$\dot{\varepsilon} = \dot{\varepsilon}_0 \, \sigma^n \exp\left(-\frac{Q}{kT}\right) \tag{1}$$

where, $\dot{\varepsilon}_0$ is a constant, n is the stress exponent, Q is the activation energy, k is the Boltzmann constant, and T the absolute temperature. In pure UO_2, the stress exponents n are about 2 at low stresses and about 5 at higher stresses. The transition stress is around 40 MPa, which means that the power-law creep mechanism becomes more activated in the region of stresses higher than 40 MPa. This value is similar to previous results [4].

The creep rate of the 0.07 wt% SCC-added samples is at least 2.3 times lower than that of pure UO_2, with its
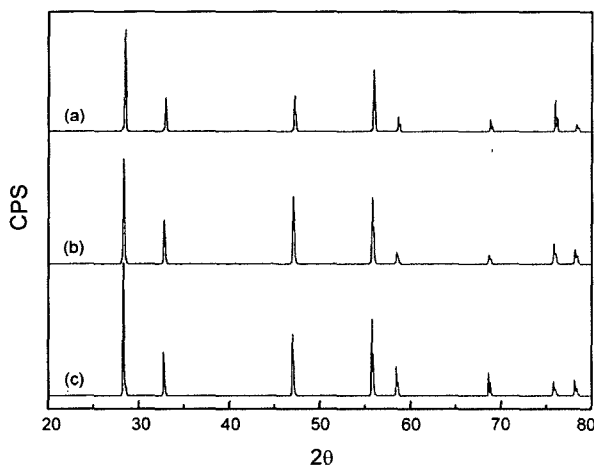
slope being the same as that of the pure UO_2 sample for the stresses of 20 and 35 MPa. This lower creep rate could be attributed to a chemical effect rather than a grain size effect, because pure UO_2 and the 0.07 wt% SCC-added UO_2 samples have similar grain sizes of about 8 μm. It seems that the glassy intergranular phase shows little contribution to the creep rate because of its insufficient fraction of the 0.07 wt% added samples.

EDS analysis results show the different Ca/Si ratios before and after sintering. The Ca/Si ratio of the initial additive is 1.006. In the second phase region of the sintered pellet, the Ca/Si ratios are changed to 0.632, 0.534, and 0.518 for the 0.07 wt%, 0.22 wt%, and 0.35 wt% added samples, respectively. The Ca/Si ratios in the UO_2 grains of the sintered pellet are 1.57, 1.39, and 1.18 for the 0.07 wt%, 0.22 wt%, and 0.35 wt% added samples, respectively. This means that CaO can be more easily dissolved into the UO_2 grains than SiO_2. Armstrong and Irvine [5] reported that a small addition of CaO reduced the creep rate relative to that of the stoichiometric UO_2. Knorr et al. [3] noted that CaO could plausibly reduce the effective value of nonstoichiometry, x, and thus may reduce the boundary diffusivity.

Figure 6 shows that the creep rate of the 0.22 wt% SCC-added UO_2 samples substantially increased and that the stress exponent is about 1 at low stresses. The creep rate of 0.22 wt% SCC-added UO_2 was about 3.48 times faster than that of pure UO_2 at 20 MPa. This increase in the creep rate might be associated with the increase in the amount of the amorphous intergranular phases. Solomon et al. [12] reported that the amorphous phases in the triple junctions could provide a continuous diffusion path between the grain edges. The slope for the 0.22 wt%
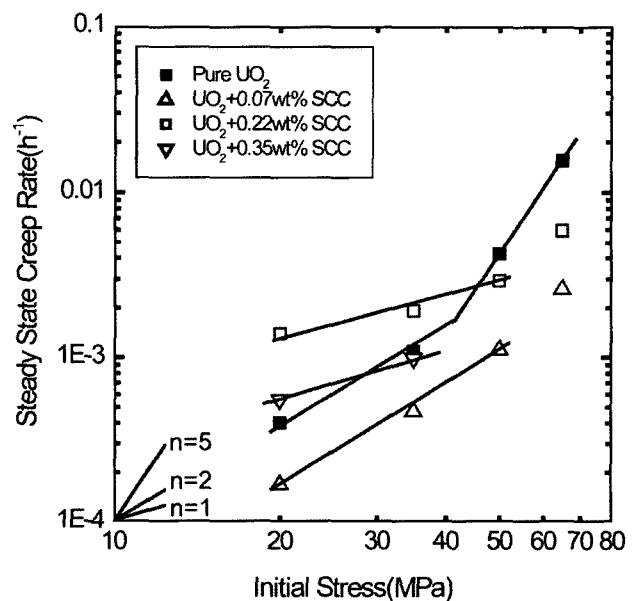

Fig. 5. X-ray Diffraction Patterns of (a) 0.07 wt%, (b) 0.22 wt% and (c) 0.35 wt% SCC-added UO_2 Samples

Fig. 6. Steady-state Creep Rates as a Function of the Applied Stress

SCC-added UO₂ samples is found to correspond with those of previous results for viscous creep [12,17]. In a polycrystal containing a glassy grain boundary phase, the cubic grain model predicts that the creep rate increases in proportion to the cube of the nominal volume fraction of a glassy phase for a linear viscous glassy phase [17]. It is likely that a sufficient amorphous intergranular phase results in a viscous creep and overcomes the chemical effect.

The viscosity of the intergranular phase, the melting point of which was estimated to be about 1540°C, as shown in Fig. 2, may be low enough to affect the creep rate at 1500°C. The contribution of the intergranular phase probably becomes more significant as the phase covers the grain faces. However, the 0.35 wt% SCC-added UO₂ samples, in spite of the large intergranular phase, show a lower creep rate than the 0.22 wt% SCC-added UO₂ samples. The creep rate is similar to that of the pure UO₂ samples. This low creep rate could result from the large grain size of the 0.35 wt% SCC-added UO₂ samples.
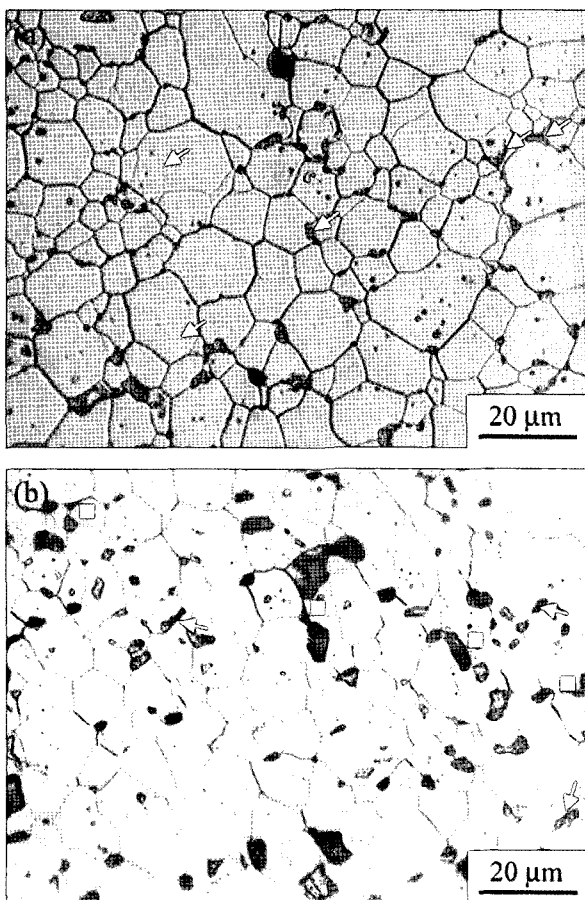
Figure 7 shows the microstructures of the pure UO₂

Fig. 7. Damage in the creep-tested samples at 50 MPa; (a) Pure UO₂, (b) 0.22 wt% SCC-added UO₂. Arrows indicate the cavities and sub-boundaries. Squares indicate crack opening.

and 0.22 wt% SCC-added samples after being deformed at 50 MPa up to 8% and 10%, respectively. Damaged areas in the pure UO₂ samples are mainly cavities and sub-boundaries. Cavities and crack openings are more clearly observed in the 0.22 wt% SCC-added sample. Grain boundary cavities suggest that the grain boundary sliding operates more significantly in the deformations of both samples. On the other hand, the sub-boundaries and higher slope in Fig. 6 suggest that dislocation creep becomes the dominant mechanism at 50 MPa in the pure UO₂ sample.

4. CONCLUSIONS

The effects of silica-based additives on the microstructure and the creep properties of a UO₂ pellet have been investigated. Among the four candidate silica-based additives, SCC (50SiO₂-47CaO-3Cr₂O₃) was selected, due to the small dihedral angle and the uniform distribution of the second phase. The creep rate of 0.22 wt% SCC-added UO₂ was about 3.48 times faster than that of pure UO₂, depending on the applied stress. The increase in the creep rate may be attributed to the enhanced diffusivity through the amorphous intergranular phases and to the low viscosity of the second phase. In the case of 0.35 wt% SCC-added UO₂, the creep rate decreased in comparison with the 0.22 wt% SCC-added UO₂, due to grain size of the 0.35 wt% SCC-added UO₂ being three times larger than those of the pure UO₂ and the 0.22 wt% SCC-added UO₂. The appropriate additive content should be determined by simultaneously considering the effects of the viscous intergranular phase and of the grain growth caused by the additives.

Acknowledgement

REFERENCES

[1] W.M. Armstrong, A.R. Causey and W.R. Sturrock, "Creep of Single-Crystal UO₂," *J. Nucl. Mater.*, **19**, 42 (1966).

[2] J.L. Routbort and J.C. Voglewede, "Creep of Mixed-Oxide Fuel Pellets at High Stress," *J. Am. Ceram. Soc.*, **56**, 330 (1973).

[3] D.B. Knorr, R.M. Cannon and R.L. Coble, "An Analysis of Diffusion and Duffusional Creep in Stoichiometric and Hyperstoichiometric Uranium Dioxide," *Acta Metal.*, **37**, 2103 (1989).

[4] F. Dherbey, F. Louchet, A. Mocellin and S. Leclercq, "Elevated Temperature Creep of Polycrystalline Uranium Dioxide," *Acta Mater.*, **50**, 1495 (2002).

[5] M.S. Seltzer, A.H. Clauer and B.A. Wilcox, "The influence of stoichiometry on compression creep of uranium dioxide single crystals," *J. Nucl. Mater.*, **44**, 43 (1972).

[6] M.S. Seltzer, A.H. Clauer and B.A. Wilcox, "The Influence

of Stoichiometry on Compression Creep of Polycrystalline UO$_{2+x}$," *J. Nucl. Mater.*, **44**, 331 (1972).

[7] W.M. Armstrong, W.R. Irvine and R.H. Martinson, "Creep Deformation of Stoichiometric Uranium Dioxide," *J. Nucl. Mater.*, **7**, 133 (1962).

[8] B. Burton, G.L. Reynolds, J.P. Barnes, "The Influence of Grain Size on the Creep of Uranium Dioxide," *J. Mater. Sci.*, **8**, 1690 (1973).

[9] T.E. Chung and T.J. Davies, "The Superplastic Creep of Uranium Dioxide," *J. Nucl. Mater.*, **79**, 143 (1979).

[10] W.M. Armstrong and W.R. Irvine, "Creep of Urania Base Solid Solutions," *J. Nucl. Mater.*, **12**, 261 (1964).

[11] Ch. Delafoy, P. Blanpain, S. Lansiart, Ph. Dehaudt, G. Chiarelli and R. Castelli, "Advanced PWR Fuels for High Burn-up Extension and PCI Constraint Elimination," *Proceedings of IAEA Technical Meeting on Improved Fuel Pellet Materials and Designs.*, pp. 163-173, October, 2003, Brussels, Belgium.

[12] A.A. Solomon, C.S. Yust and N.H. Packan, "Primary Creep of UO₂ and the Effect of Amorphous Grain Boundary Phases," *J. Nucl. Mater.*, **110**, 333 (1982).

[13] K.W. Lay, H.S. Rosembaum, J.H. Davis and M.O. Marlowe, "Nuclear Fuel," US Pat. 4869866 (1989).

[14] K.W. Lay, H.S. Rosembaum and J.H. Davis, "Nuclear Fuel," US Pat. 4869867 (1989).

[15] K.W. Kang, J.H. Yang, K.S. Kim, J.H. Kim and K.W. Song, "Effect of Additives on Creep Property of UO₂ Pellet," *Proceedings of the Kor. Nucl. Soc.*, Spring Meeting, May 2001.

[16] Y.K. Bibilashvili, F.G. Reshetnikov, V.V. Novikov, A.V. Medvedev, O.V. Milovanov, A.V. Kuleshov, E.N. Mikheev, V.I. Kuznetsov, V.B. Malygin, K.V. Naboichenko, A.N. Sokolov, V.I. Tokarev and Y.V. Pimenov, "Development of Low-Strain Resistant Fuel for Power Reactor Fuel Rods," *Proceedings of IAEA Technical Meeting on Improved Fuel Pellet Materials and Designs.*, pp.297-305, October, 2003, Brussels, Belgium.

[17] D.S. Wilkinson, "Creep Mechanisms in Multiphase Ceramic Materials," *J. Am. Ceram. Soc.*, **81**, 275 (1998).

[18] Levin, E. M., Robbins, C. R. and McMurdie, H. F., Figs. 101, 302, 651 and 2388 in *Phase Diagrams for Ceramists*, ed. by M. K. Reser. American Ceramic Society, Columbus, OH, 1964.